Earth and Planetary Science Letters 419 (2015) 168–177

Contents lists available at ScienceDirect

Earth and Planetary Science Letters

www.elsevier.com/locate/epsl

Tungsten isotope composition of the Acasta Gneiss Complex

M. Willbold [a,b,*], S.J. Mojzsis [c,d,e], H.-W. Chen [a], T. Elliott [a]

[a] School of Earth Sciences, Bristol Isotope Group, University of Bristol, Wills Memorial Building, Queen's Road, Bristol BS8 1RJ, United Kingdom
[b] School of Earth, Atmospheric and Environmental Sciences, Isotope Geochemistry & Cosmochemistry Group, University of Manchester, Oxford Road, Manchester M13 9PL, United Kingdom
[c] Department of Geological Sciences, NASA Lunar Science Institute Center for Lunar Origin and Evolution (CLOE), University of Colorado, UCB 399, 2200 Colorado Avenue, Boulder, CO 80309-0399, USA
[d] Laboratoire de Géologie de Lyon, École Normale Supérieure de Lyon and Université Claude Bernard Lyon 1, CNRS UMR 5276, 46 Allée d'Italie, 69007 Lyon, France
[e] Hungarian Academy of Sciences, Research Center for Astronomy and Earth Sciences, Institute for Geological and Geochemical Research, Budaörsi ut 45, H-1112 Budapest, Hungary

ARTICLE INFO

Article history:
Received 6 September 2014
Received in revised form 18 February 2015
Accepted 23 February 2015
Available online 18 March 2015
Editor: B. Marty

Keywords:
Archean
mantle
crust
late veneer
tungsten isotopes
Acasta Gneiss Complex

ABSTRACT

High-precision tungsten ($^{182}W/^{184}W$) isotope measurements on well-characterised mafic and felsic samples of the ca. 3960 Ma Acasta Gneiss Complex (AGC; Northwest Territories, Canada) show radiogenic $\varepsilon^{182}W$ values between +0.06 to +0.15. Two ca. 3600 Ma felsic samples from this terrane have $\varepsilon^{182}W \sim 0$ and are the oldest samples so far documented to have a W isotopic composition indistinguishable from that of the modern mantle. The $\varepsilon^{182}W$ data are correlated with $\varepsilon^{142}Nd$ (Roth et al., 2014) and we attribute this variability to incomplete metamorphic homogenisation of the 3960 Ma protolith with more recent material in a 3370 Ma tectono-thermal event. Notably, the value of the positive $\varepsilon^{182}W$ anomalies seen in the 3960 Ma AGC samples that are least affected by metamorphic homogenisation is comparable to that observed in other early Archean rocks (Isua Supracrustal Belt, Greenland; Nuvvuagittuq Supracrustal Belt, Canada) and the late Archean Kostomuksha komatiites (Karelia). This demonstrates a globally constant signature. We infer that the presence of a pre-late veneer mantle represents the most straightforward interpretation of a uniform distribution of $\varepsilon^{182}W \sim +0.15$ value in Archean rocks of different ages. We show that such a notion is compatible with independent constraints from highly siderophile element abundances in mafic and ultra-mafic Archean mantle-derived rocks. The absence of anomalous $\varepsilon^{182}W$ and $\varepsilon^{142}Nd$ so far measured in samples younger than ca. 2800 Ma suggests progressive convective homogenisation of silicate reservoirs. The downward mixing of an upper mantle rich in late-delivered meteoritic material might account for these combined observations.

1. Introduction

Seismic tomography and geochemical constraints provide us with a detailed picture of the physical and dynamic state of the present-day mantle (Coltice and Schmalzl, 2006; Kellogg and Turcotte, 1990; van der Hilst, 1999; van Keken and Zhong, 1999). Valuable information on the geodynamic regimes prevalent on the early Earth can be obtained by numerical simulations and analogue experiments (e.g. Davaille, 1999; Gonnermann et al., 2002; Samuel and Farnetani, 2003). Yet, uncertainties about physical parameters that characterised the Earth's initial planetary conditions make it difficult to quantitatively assess the early Earth's convective regimes. Observational evidence to constrain the dynamics of the terrestrial Archean mantle has been scant, but high-precision determinations of differences in $^{142}Nd/^{144}Nd$ resulting from decay of short-lived ^{146}Sm have recently opened a new window into the evolution of Hadean-early Archean rocks (e.g. Bennett et al., 2007; Boyet et al., 2003; Caro et al., 2003; Debaille et al., 2013; O'Neil et al., 2008; Rizo et al., 2011; Roth et al., 2013). Investigating how early-formed reservoirs with discrete $^{146}Sm/^{144}Nd$ were dispersed and homogenised within the Earth over geological time-scales yields important information on the physical structure of the early terrestrial mantle (Bennett et al., 2007; Caro et al., 2003, 2005; Debaille et al., 2013; Harper and Jacobsen, 1992; Rizo et al., 2013).

The short-lived ^{182}Hf–^{182}W system offers a further powerful means to probe Earth's formation and early evolution. With a half-life of 8.9 Myr (Vockenhuber et al., 2004) variations in $^{182}W/^{184}W$ can only have been produced during the first ca. 50 million years

* Corresponding author at: School of Earth, Atmospheric and Environmental Sciences, Isotope Geochemistry & Cosmochemistry Group, University of Manchester, Oxford Road, Manchester M13 9PL, United Kingdom.
E-mail address: matthias.willbold@manchester.ac.uk (M. Willbold).

http://dx.doi.org/10.1016/j.epsl.2015.02.040

of solar system history. The siderophile character of W compared to the lithophile behaviour of its parent Hf (Goldschmidt, 1930) means that significant amounts of Earth's W were sequestered into the core. That the Earth's mantle has a $^{182}W/^{184}W \sim 200$ ppm higher than chondritic meteorites implies this process occurred while ^{182}Hf was still extant (Kleine et al., 2002; Schoenberg et al., 2002; Yin et al., 2002). This pervasive planetary process dominates the terrestrial W isotopic composition. More recently, well-resolved ~15 ppm enrichments in $^{182}W/^{184}W$ relative to the present-day mantle value were discovered in ca. 3800 Ma early Archean rocks from the Isua Supracrustal Belt in southern West Greenland (Willbold et al., 2011). The authors postulated that the magnitude of positive $^{182}W/^{184}W$ anomalies observed in the Isua Supracrustal Belt is consistent with the estimated W isotopic composition of a Hadean mantle prior to the addition of a chondritic 'late veneer' (Chou, 1978; Morgan, 1985). In the model favoured by Willbold et al. (2011), the discrepancy between the W isotope budget of Hadean and the present-day mantle is therefore reconciled by externally augmenting the Earth with chondritic material sometime between the giant Moon-forming impact and the purported "Late Heavy Bombardment" (Tera et al., 1974). If this interpretation is correct, high-precision W isotope data may be used to trace how this chondritic material mixed into the Hadean/Archean mantle and thus provide useful insights into the geodynamic framework of the early terrestrial mantle.

In contrast, others (Touboul et al., 2014, 2012) have attributed terrestrial $\varepsilon^{182}W$ anomalies to very early silicate differentiation processes or continued silicate-metal fractionation after core formation ($\varepsilon^{182}W$ is the part-per-ten thousand deviation of the measured $^{182}W/^{184}W$ in a sample relative to that of the standard, i.e. the modern mantle value). In the case of the Touboul et al. (2012) model, the higher incompatibilities of W and Nd relative to Hf and Sm for most silicate solids might predict elevated $\varepsilon^{142}Nd$ to be associated with positive $\varepsilon^{182}W$. This is indeed the case for the Isua Supracrustal Belt, although Willbold et al. (2011) showed that the magnitudes of the two anomalies were inconsistent with the simplest model scenarios. It is thus of significant interest to examine early Archean samples with negative $\varepsilon^{142}Nd$, where a negative $\varepsilon^{182}W$ might be expected as a corollary of early silicate differentiation as suggested by Touboul et al. (2012).

Touboul et al. (2014) have recently investigated samples with negative $\varepsilon^{142}Nd$ from the early Archean Nuvvuagittuq Supracrustal Belt (NSB) in northern Québec (Canada), but these samples show a positive $\varepsilon^{182}W \sim +0.15$ anomaly similar to the samples from the Isua Supracrustal Belt (Willbold et al., 2011). To account for these differences, in conjunction with the samples' siderophile element abundances, Touboul et al. (2014) argue for a decoupling of $\varepsilon^{182}W$ from $\varepsilon^{142}Nd$ as a result of the preferential mobility of W in subduction related fluids. Here, we examine further the relationship between $\varepsilon^{142}Nd$ and $\varepsilon^{182}W$ values, with high-precision W isotope analyses of 3600 to 3960 Ma (Mojzsis et al., 2014) Archean rocks from the Acasta Gneiss Complex (AGC), Northwest Territories (Canada). Our study includes samples with negative $\varepsilon^{142}Nd$, suggestive of a Hadean silicate differentiation event (Roth et al., 2014).

2. Geological background, previous data and sample selection

Details of the geological setting for all samples analysed in this study are reported in Mojzsis et al. (2014), Guitreau et al. (2014) and Roth et al. (2014) and in the Supplementary Material. Only a brief overview is provided here summarising information relevant for the interpretation of our data. Detailed field studies (Iizuka et al., 2006, 2009, 2007) have identified four dominant lithologies within the AGC (mafic, felsic, layered and foliated series). Samples of this study belong to two of these groups: (i) the mafic series comprising gabbroic, quartz dioritic and dioritic

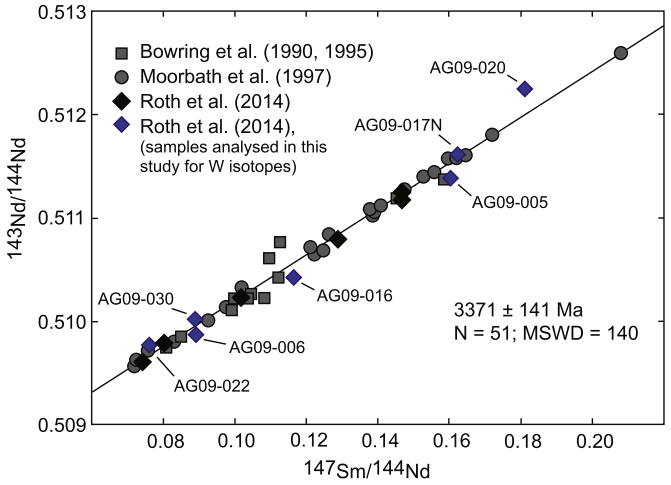

Fig. 1. $^{143}Nd/^{144}Nd$–$^{147}Sm/^{144}Nd$ errorchron for Acasta Gneiss Complex samples (Bowring and Housh, 1995; Bowring et al., 1990; Moorbath et al., 1997; Roth et al., 2014). Samples analysed for $^{182}W/^{184}W$ isotopes in this study are shown in blue and are labelled. The data has been interpreted as the result of partial re-equilibration of the ^{147}Sm–^{143}Nd isotope system at ca. 3370 Ma (Roth et al., 2014) due to a pervasive metamorphic event as documented by secondary zircon growth (Mojzsis et al., 2014; Moorbath et al., 1997; Roth et al., 2014; Whitehouse et al., 2001).

gneisses and (ii) the felsic series consisting of tonalitic, trondhjemitic, granodioritic and granitic gneisses. Although much older, ca. 4200 Ma zircon xenocrysts were previously identified in felsic gneisses (Iizuka et al., 2006), the dominant age of magmatic zircons in felsic gneisses that are in chemical equilibrium with their host rock are of ca. 3960 Ma age (Mojzsis et al., 2014). The latter age most likely represents the time of the emplacement of the AGC (Mojzsis et al., 2014). Younger, ca. 3600 Ma concordant ages from felsic gneiss samples were attributed to zircon growth in amphibolite grade metamorphic events as well as crust addition to the AGC (Bowring and Housh, 1995; Guitreau et al., 2012; Iizuka et al., 2007; Mojzsis et al., 2014).

Roth et al. (2014) and Guitreau et al. (2014) reported combined $^{142}Nd/^{144}Nd$, $^{143}Nd/^{144}Nd$ and $^{176}Hf/^{177}Hf$ data for AGC samples reported in Mojzsis et al. (2014). Most samples show a deficit in $^{142}Nd/^{144}Nd$ of up to −14 ppm relative to present-day mantle, in line with the formation and isolation of an early enriched reservoir in the Hadean and a late Hadean/early Archean emplacement age for these rocks (Roth et al., 2014). Combined ^{147}Sm–^{143}Nd data for these samples, however, define a 3370 Ma Mesoarchean errorchron (Fig. 1) similar to previous findings (Mojzsis et al., 2014; Moorbath et al., 1997; Whitehouse et al., 2001). This discrepancy was attributed to partial resetting of the ^{147}Sm–^{143}Nd and ^{146}Sm–^{142}Nd systems during a 3370 Ma metamorphic event (Roth et al., 2014). Based on combined whole-rock $^{176}Hf/^{177}Hf$, U–Pb zircon and trace element data, Guitreau et al. (2014) concluded that gneisses belonging to the 3960 Ma age group were derived from mantle melts with only limited contributions from pre-existing crustal material. Notably, the same samples also display well-resolved deficits in $^{142}Nd/^{144}Nd$ (Roth et al., 2014). Felsic gneisses of the 3600 Ma U–Pb zircon age group show modern terrestrial $^{142}Nd/^{144}Nd$ values (Roth et al., 2014) and crustal $^{176}Hf/^{177}Hf$ ratios (Guitreau et al., 2014) indicating that these samples derived, at least in part, from crust with a $^{142}Nd/^{144}Nd$ similar to that of modern bulk silicate Earth.

For this study, samples were earmarked for W isotope analysis (Fig. 1) based on a desire to cover a wide range of Nd and Hf isotope compositions (Guitreau et al., 2014; Roth et al., 2014) as well as simple age spectra (Guitreau et al., 2012; Mojzsis et al., 2014). Thus, we analysed four felsic gneisses that belong to the 3960 Ma

age group, AG09-005, -006, -016, -030, where the latter two samples were dated by U–Pb zircon data and the others are associated from field relationships (Guitreau et al., 2014; Mojzsis et al., 2014; Roth et al., 2014). Two mafic gneisses were analysed, AG09-017N and -020. Field observations suggest that several generations of felsic gneisses enclose and dismember the mafic gneiss complexes from which these two samples were derived (Guitreau et al., 2014). Consequently, it has been suggested that the mafic gneisses are the oldest rocks of the AGC (Bleeker and Stern, 1997) and we therefore attribute these two samples to the 3960 Ma group. Two 3600 Ma felsic gneisses (AG09-015 and -022) were analysed.

3. Methods

To quantitatively separate W from matrix elements, about 5 g of sample powder were processed through an alkaline chemical separation procedure as detailed in Willbold et al. (2011). For mass spectrometric analyses, the samples were dried down and re-dissolved in 0.4 M HNO_3–0.4 M HF. Concentrations of W in the final solutions were adjusted to match (to within 10%) the 400 ng/mL NIST SRM 3136 W standard solution used for sample-standard bracketing. Total procedural blanks were determined to be <1 ng W (for a procedure equivalent to that used for processing 5 g of sample powder) and are negligible compared to >500 ng typically used for analysis. Measurements were performed on a ThermoFinnigan Neptune multi-collector ICPMS (serial No. 1020) at the University of Bristol using the protocols as detailed in Willbold et al. (2011). Typical sensitivity was ca. 4500 pA for a 1 µg/mL W solution, using "X" skimmer cones, standard sampler cones, standard rotary interface pump and 50 µL/min nebulizer. Accuracy and reproducibility of the method set-up (chemical separation and mass spectrometric analysis) were tested by repeated measurements of La Palma basalt LP-68d and the CPI W standard (both $N = 4$). The results are shown in Table 1 and agree well with data for other terrestrial Phanerozoic samples (Touboul et al., 2014, 2012; Touboul and Walker, 2012; Willbold et al., 2011). W concentrations were measured by isotope dilution, on separate splits of the powders analysed for $^{182}W/^{184}W$ ratios, using a ^{183}W tracer, calibrated against NIST SRM 3163 and measured on a ThermoFinnigan Neptune multi-collector ICPMS (serial No. 1002). Additional details of the analytical setup are given in the Supplementary Material.

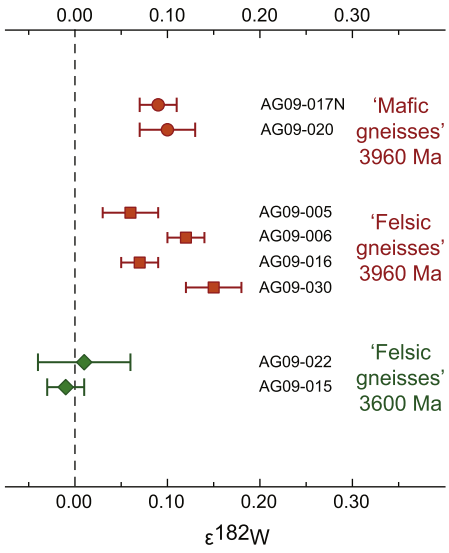

Fig. 2. Tungsten (W) isotope composition of samples from the Acasta Gneiss Complex. The data ($\varepsilon^{182}W$) is reported in parts-per-10 000 deviation of $^{182}W/^{184}W$ in samples relative to that of NIST SRM 3136 ($\varepsilon^{182}W = 0$). Errors are given as $2\sigma_m$. Data is subdivided into three petrological and age groups: mafic and felsic gneisses of 3960 Ma age (red) and 3600 Ma felsic gneisses (green).

4. Results

The AGC whole-rock W isotope data for the six felsic gneisses and two mafic gneisses are reported in Table 1 and Fig. 2. Measured W concentrations and W/Th ratios are given in Table 1 and are shown in Fig. 3. All AGC samples belonging to the 3960 Ma group have positive $\varepsilon^{182}W$ anomalies relative to present-day mantle and range between $\varepsilon^{182}W$ +0.06 to +0.15 (Fig. 2). Samples AG09-015 and -022, belonging to the younger 3600 Ma age group have $\varepsilon^{182}W$ indistinguishable from that of the present-day mantle. Most samples of the 3960 Ma age group have $\varepsilon^{142}Nd$ between −0.09 and −0.13. Sample AG09-030 with the highest $\varepsilon^{182}W$ +0.15 has the lowest $\varepsilon^{142}Nd$ (−0.14; Fig. 4). In contrast, 3600 Ma sample AG09-022 has an $\varepsilon^{142}Nd$ value indistinguishable from the present-day mantle and also comprises $\varepsilon^{182}W \sim 0$ (Fig. 4). No $\varepsilon^{142}Nd$ value for sample AG09-015 is available, but as shown by

Table 1
W isotopic composition of Archean samples from the Acasta Gneiss Complex and reference materials.

Sample	Lithology[a]	Age group (Ma)[a,b,c]	$\varepsilon^{182}W$	2 s.e.[d]	$\varepsilon^{183}W$	2 s.e.	W (µg/g)	Th (µg/g)[a]	W/Th	$\varepsilon^{142}Nd$[c]	2 s.e.
AG09-005	felsic gneiss	3960	0.06	0.03	−0.05	0.03	0.108			−0.09	0.02
AG09-006_1			*0.12*	*0.02*	*0.00*	*0.02*					
AG09-006_2			*0.12*	*0.02*	*−0.04*	*0.03*					
AG09-006 ave	felsic gneiss	3960	0.12	0.02	−0.02	0.02	0.556				
AG09-016	felsic gneiss	3960	0.07	0.02	0.00	0.02	0.302	19.2	0.0158	−0.12	0.02
AG09-17N	mafic gneiss	3960	0.09	0.02	0.00	0.02	0.974	0.498	1.96	−0.09	0.04
AG09-020_1			*0.10*	*0.02*	*0.01*	*0.02*					
AG09-020_2			*0.11*	*0.03*	*−0.01*	*0.02*					
AG09-020 ave	mafic gneiss	3960	0.10	0.02	0.00	0.02	2.30	0.888	2.59	−0.10	0.04
AG09-030	felsic gneiss	3960	0.15	0.02	−0.02	0.02	0.319			−0.14	0.03
AG09-015[f]	felsic gneiss	3600	−0.01	0.02	−0.01	0.02	0.228	19.7	0.0116	0.01[f]	0.04
AG09-022	felsic gneiss	3600	0.01	0.05	−0.06	0.07	0.755			0.03	0.02
		$N =$	$\varepsilon^{182}W$	2 s.d.[e]	$\varepsilon^{183}W$	2 s.d.					
Average LP-68d	La Palma basalt[g]	4	0.01	0.02	−0.01	0.03					
Average CPI W standard	W ICP standard[g]	4	0.00	0.04	−0.01	0.03					

[a] Mojzsis et al. (2014).
[b] Guitreau et al. (2014).
[c] Roth et al. (2014).
[d] 2 s.e.: 2 sigma error.
[e] 2 s.d.: 2 standard deviation.
[f] $\varepsilon^{142}Nd$ value taken as average of 3600 Ma group in Roth et al. (2014).
[g] See Willbold et al. (2011) for sample details.

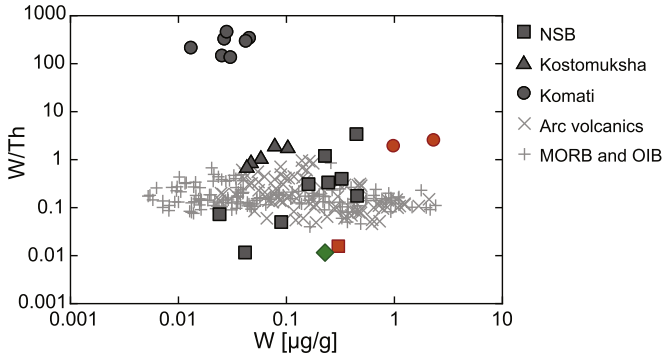

Fig. 3. W/Th ratios plotted against W concentrations for samples of this study (same symbols as in Fig. 2). Also shown are data for samples from the Nuvvuagittuq Supracrustal Belt (NSB) and Kostomuksha komatiites that comprise radiogenic ε^{182}W values as well as Komati komatiites (Touboul et al., 2014, 2012). Data for arc volcanics, ocean island basalts (OIB) and mid-ocean ridge basalts (MORB) are shown for reference (Arevelo and McDonough, 2008; König et al., 2011, 2008). Note the overlap of W/Th ratios in Archean terranes – in particular those of late Archean komatiites (Kostomuksha) and early Archean supracrustal terranes (AGC, NGB) – as well as their large range and high values compared to post-Archean rocks. See text for discussion.

Roth et al. (2014), gneisses of the 3600 Ma age group display consistently uniform ε^{142}Nd values close to the present-day mantle value. We therefore assume an ε^{142}Nd of -0.01 ± 0.04 (i.e. the average value of ca. 3600 Ma old samples reported by Roth et al. (2014) for sample AG09-015. The eight gneiss samples from our study thus define a loose negative trend in ε^{182}W–ε^{142}Nd space (Fig. 4). Notably, samples of both major lithologies, 3960 Ma mafic *and* felsic gneisses (i.e. AG09-020, AG09-017N and AG09-030), display excess ε^{182}W values and deficits in ε^{142}Nd relative to present-day mantle.

5. Discussion

5.1. The ε^{182}W signature of the Acasta Gneiss Complex

The AGC samples display a significant spread in ε^{182}W ranging from -0.01 to $+0.15$, with positive ε^{182}W only displayed in the oldest, 3960 Ma samples. Sample AG09-030 resembles an end member as it not only has the most positive ε^{182}W of $+0.15$ but also the most negative ε^{142}Nd (Fig. 4) and may thus approach the primary W isotopic composition of the AGC. Most notably, a value of $+0.15$ is within error of the ε^{182}W anomalies in the two other early Archean terranes analysed to date (i.e. the Isua Supracrustal Belt and the NSB; Fig. 5).

A magmatic age of the 3960 Ma group has been established, but detailed U–Pb data for the whole zircon population in these samples also indicate systematic Pb-loss as a result of protracted metamorphic reworking during the Archean (Mojzsis et al., 2014). Some 3960 Ma samples may thus have been contaminated by later addition of W with $\varepsilon^{182}\text{W} = 0$ during post-emplacement metamorphism. A partial overprinting of the ε^{182}W signature in 3960 Ma AGC samples is consistent with a model presented by Roth et al. (2014) who suggested that ε^{142}Nd and ε^{143}Nd for the same sample set has been partially reset during a 3370 Ma crustal reworking processes (Fig. 1).

Intracrustal fluid migration is an important parameter in controlling the bulk-transport of elements within the Earth's crust. In particular, the chemical composition of pegmatites in high-grade metamorphic/magmatic terranes demonstrates that fluids associated with such high-grade systems are enriched in incompatible elements; e.g. see Linnen et al. (2012) and references therein. Experimental data suggests that at crustal pressures and temperatures, W is concentrated in the fluid phase of granitic melt-vapour systems (Manning and Henderson, 1984). Such high solubility (fluid/solid distribution coefficients of $D^{f-s} > 0.6$ and most commonly larger than 1 with values up to 6) is in line with the observation that hydrothermal W ore deposits are often associated with granitic intrusions (Audétat et al., 2000; Raith and Prochaska, 1995). For instance, W ore mineralisations commonly associated with porphyry Cu–Mo–Au deposits are almost exclusively epigenetic and thus secondary to their host rocks (Herrington, 2011). Recent geochemical constraints of W mobility in high-pressure, high-temperature fluids suggest that W may be up to three times more mobile than U in high-grade metamorphic fluids (Bali et al., 2012; König et al., 2008). Using these constraints, the effect of W and Nd mobility during metamorphic overprinting can be evaluated for our samples (Fig. 4). No consistent dataset of D^{f-s} values exists for W and Nd. Here, we conservatively assume a low D^{f-s} value of 0.9 for W (König et al., 2008; Manning and Henderson, 1984) and 0.3 for Nd in metamorphic fluids at crustal conditions (Masters and Ague, 2005; Ordóñez Calderón et al., 2008). The results show, that the variation of ε^{182}W–ε^{142}Nd in AGC samples can be accounted for by the addition of 'modern' terrestrial W and Nd isotopic compositions in proportions carried by metamorphic fluids to the 3960 Ma crust. Note that the use of different D^{f-s} values in this calculation would change the curvature of the calculated mixing trend, but it would remain convex down given that the mobility of W will always be higher than that of Nd (Audétat et al., 2000; Manning and Henderson, 1984; Masters and Ague, 2005; Ordóñez Calderón et al., 2008; Raith and Prochaska, 1995). While we assume a simple batch-mixing model here for simplicity, re-equilibration with an external fluid would yield a similar mixing relationship. No correlation of ε^{182}W with W concentrations is anticipated for our dataset given that the primary W concentrations of these felsic samples is similar to that in the metamorphic fluid (i.e. $D^{f-s} = 0.9$; see caption of Fig. 4 and Supplementary Material).

Our interpretations reflect the susceptibility of W isotope systematics in early Archean terranes to partial resetting during post-emplacement metamorphic events. Previous reports of positive ε^{182}W anomalies in such ancient terranes have come from the Isua Supracrustal Belt (Willbold et al., 2011) and NSB (Touboul et al., 2014). Although both localities have suffered subsequent metamorphic over-printing, we suggest that the near constant positive

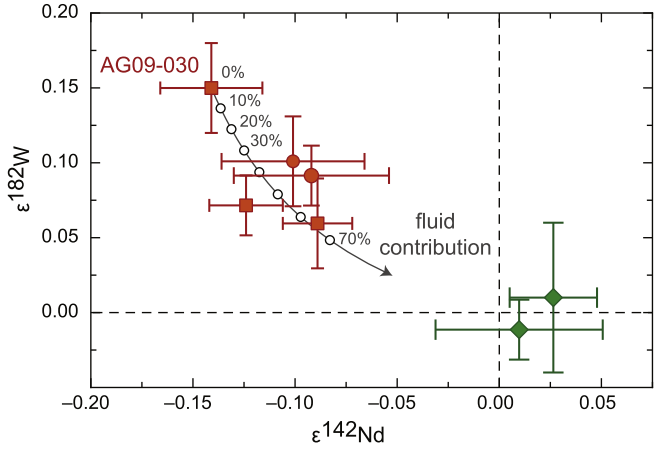

Fig. 4. Combined ε^{182}W–ε^{142}Nd data for samples of this study. ε^{142}Nd data taken from Roth et al. (2014). Errors are given as $2\sigma_m$. Same symbols as in Fig. 2. For sample AG09-015 an ε^{142}Nd of -0.01 is assumed (i.e. the average value of 3600 Ma samples reported by Roth et al., 2014; see text). The solid curve shows the effect of fluid addition to 3960 Ma felsic protocrust. Note that the two mafic gneiss samples AG09-020 and -017N are enriched in W and may have been affected by the 3370 Ma metamorphic fluid influx to a lesser degree than the felsic gneisses. Sample AG09-030 displays the largest excess in ε^{182}W and highest deficit in ε^{142}Nd and, accordingly, is assumed to represent the least altered sample affected by this event. Details of the model calculation are given in the Supplementary Material.

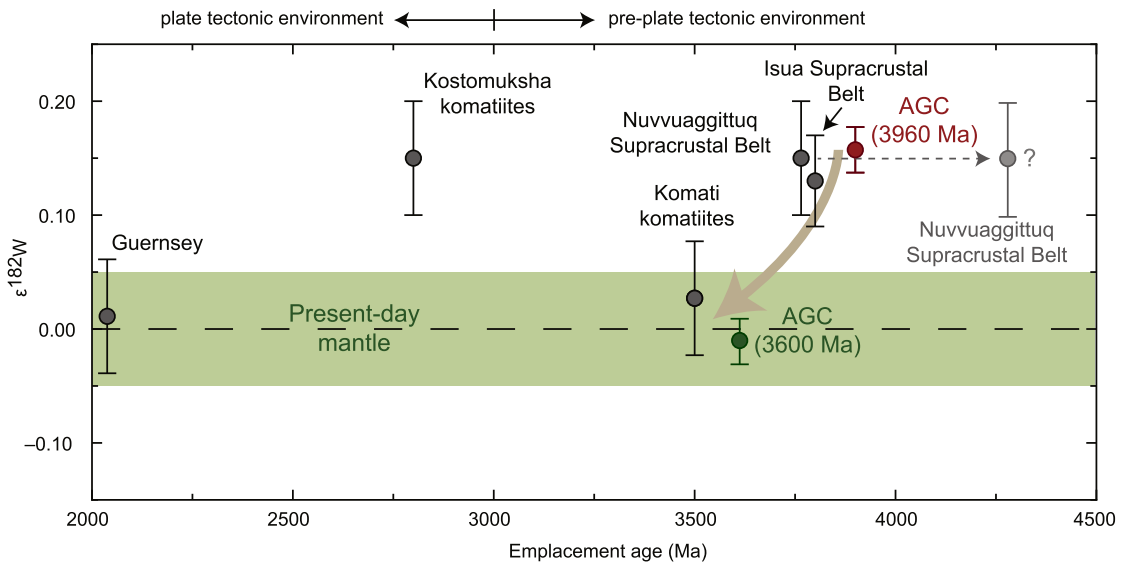

Fig. 5. Average ε^{182}W in Hadean to Proterozoic rocks plotted against magmatic emplacement age. Note the saw-tooth pattern formed by ε^{182}W data over time with maxima at 3800 and 2800 Ma. See text for discussion. Literature data taken from Willbold et al. (2011) for the Isua Supracrustal Belt and Guernsey gneiss, Touboul et al. (2012) for Kostomuksha and Komati komatiites, Touboul et al. (2014) for the Nuvvuagittuq Supracrustal Belt. We assume an emplacement age of ca. 3750 Ma for the Nuvvuagittuq Supracrustal Belt (Cates and Mojzsis, 2007) although we note that assuming an older emplacement age (O'Neil et al., 2008) is not critical for our interpretation of the global ε^{182}W data.

ε^{182}W across a range of different lithologies implies that fluids may have redistributed W on the length-scale of these outcrops (~5 km) but not resulted in mixing of isotopically different W from further afield. In contrast, the oldest (3960 Ma) components of the AGC are smaller (Iizuka et al., 2006; Mojzsis et al., 2014) and more likely to have exchanged W with younger (<3600 Ma) surrounding units. Indeed, whole-rock samples from Isua Supracrustal Belt, and more contentiously from NSB, preserve evidence of their antiquity in their bulk sample isochrons, which is much less clearly retained in most AGC samples (see Fig. 1, above and Supplementary Material).

5.2. A subduction zone origin for the elevated ε^{182}W in the 3960 Ma AGC samples?

Touboul et al. (2014) recently reported positive ε^{182}W for mafic samples from the NSB, but noted that their elevated W concentrations are inconsistent with melts derived from partial melting of a primitive mantle source. They proposed that high-W fluids, derived from subducted Hadean sediments with radiogenic ε^{182}W, contaminated a mantle wedge that was characterised by a primary unradiogenic ε^{142}Nd signature and a highly siderophile element budget (HSE: Os, Ir, Ru, Pt, Pd, Re) similar to that of the present-day mantle. Our current dataset of more evolved samples, which have not been analysed for HSE abundances, does not allow us to rule out a similar model for the AGC. Nevertheless, subduction zone-related dehydration processes, such as those proposed by Touboul et al. (2014), predominantly operate in steep and cool subduction zone systems (Bali et al., 2012; König et al., 2008), which are considered unrepresentative of the Hadean–Archean Earth (Condie, 2008; Martin and Moyen, 2002; Moyen and Martin, 2012; Nair and Chacko, 2008; Shirey and Richardson, 2011; Smithies et al., 2005, 2007; Van Kranendonk, 2007; Van Kranendonk et al., 2007a, 2007b). We further note that the subduction zone model by Touboul et al. (2014) is strongly based on the generic similarity of trace element data for samples from the NSB and those form modern subduction zones. Willbold et al. (2009) cautioned against the use of trace element discrimination diagrams to decipher the tectonic setting of early Archean crustal belts. These authors stressed that some key samples from the Iceland oceanic plateau, albeit rare today, bear the breadth of 'diagnostic trace element' characteristics used as hallmarks of modern subduction zones rocks. We therefore argue that circumstantial evidence for a particular tectonic regime based solely on trace element data in Archean rocks does not provide strong constraints.

These arguments are usefully framed with relative W abundance data (Fig. 4). Our two mafic AGC samples AG09-020 and AG09-017N have W/Th ratios of 2.59 and 1.96 (Table 1), much higher than those found in present-day arc lavas and oceanic basalts (Fig. 3) but are comparable with the high W/Th ratios found in mafic rocks from the NSB. Perhaps surprisingly, the W/Th ratios of the Kostomuksha komatiites show similar W/Th enrichments to the early Archean terranes (Fig. 3), whereas even higher W/Th ratios of 137 to 465 were found in komatiites from Komati (Touboul et al., 2012). A subduction zone origin as well as crustal contamination during emplacement were firmly excluded for the two Archean komatiite suites of Kostomuksha and Komati (Puchtel et al., 1998, 2014; Touboul et al., 2012) and we therefore conclude that high W/Th ratios in mafic Archean rocks, especially from the AGC and NSB, may be an intrinsic geochemical feature of Archean mantle-derived rocks and do not seem to be indicative of a subduction zone origin.

5.3. Origin of positive ε^{182}W anomalies in the Earth's mantle

This and previous studies (Touboul et al., 2014; Willbold et al., 2011) show that positive ε^{182}W anomalies in ancient gneiss complexes are associated with both negative (AGC, NSB) and positive ε^{142}Nd anomalies (Isua Supracrustal Belt, NSB). It has been suggested that an early planetary-scale mantle differentiation event in the early Hadean caused the formation of silicate reservoirs with anomalous ε^{182}W (Touboul et al., 2012). In the simplest manifestation of this model, negative ε^{182}W would be anticipated for samples with negative ε^{142}Nd, which is neither observed in the case of the NSB (Touboul et al., 2014) nor here for the AGC. The short half-life of the ^{182}Hf–^{182}W decay system and the constraint that magmatic differentiation leading to Hf/W ratios higher than primitive mantle could only have produced supra-bulk silicate Earth Sm/Nd ratios (e.g. Iizuka et al., 2010) would require at least two,

pervasive silicate differentiation events to reconcile the present ε^{182}W–ε^{142}Nd dataset of early Archean gneiss complexes. Such a scenario is by no means implausible, but is not compellingly straightforward. Moreover, it does not account for the influence of late accretion on the evolution of terrestrial planets (e.g. Bottke et al., 2010), which we believe is a significant consideration.

We note that all gneiss complexes older than ca. 3600 Ma, in addition to the 2800 Ma Kostomuksha komatiites, yield near identical maximum ε^{182}W anomalies of ca. +0.15 (Fig. 5). We also emphasise that an ε^{182}W value of ca. +0.15 is entirely consistent with that of a pre-late veneer mantle using independent constraints from HSE abundances (Chou, 1978; Morgan, 1986; Touboul et al., 2012; Willbold et al., 2011). Given the global areal distribution of the Hadean/early Archean AGC, NSB and Isua Supracrustal Belt complexes, this pre-late veneer mantle appears to be the main source of crust formed at that time (Fig. 5). It is commonly accepted that chondritic material was delivered to the Earth during a 'late veneer' period subsequent to the giant Moon-forming impact (e.g. see Walker, 2009). The chondritic material delivered to the Hadean mantle was characterised by ε^{182}W ~ -2 relative to present-day mantle (Kleine et al., 2002; Yin et al., 2002). Mixing and homogenisation of this chondritic component in the terrestrial mantle over time then resulted in a present-day ε^{182}W = 0 for the bulk silicate Earth (Willbold et al., 2011).

While rocks older than ca. 3600 Ma show a systematic offset in ε^{182}W (Fig. 5), ca. 3500 Ma mantle-derived komatiites from the Barberton Belt (Komati) are characterised by ε^{182}W of ca. 0 (Touboul et al., 2012), identical to the modern-mantle reference (Fig. 5). In this respect, the AGC serves as a key locality where the 3960 Ma rocks preserve such a positive anomaly, whereas 3600 Ma rocks have modern ε^{182}W values making them the oldest known rocks with modern mantle-like W isotopic compositions. Notably, the contact between both rock types is purely magmatic, i.e. the 3600 Ma gneisses represented by samples AG09-015 and -022 intrude 3960 Ma gneisses (Guitreau et al., 2014). Within a time interval of less than 400 million years, the W isotopic composition of the mantle source, which supplied primary crust to the AGC, must have changed. Taken together with data from other Archean terranes (Fig. 5) this temporal decrease in ε^{182}W suggests that the meteoritic material added from the late veneer became homogenised within the mantle reservoir between 3960 and 3600 Ma. That Archean rocks with ε^{182}W > 0 are characterised by either positive and negative ε^{142}Nd, suggests that several, possibly unrelated silicate differentiation events formed different crustal and mantle reservoirs with Sm/Nd ratios higher and lower than the primitive mantle while ^{146}Sm was still extant (Bennett et al., 2007; Caro et al., 2003, 2006; O'Neil et al., 2008; Rizo et al., 2012, 2013; Roth et al., 2014, 2013) but when ^{182}Hf was already extinct.

5.4. A unifying model for W isotope and HSE constraints in Archean terranes?

Touboul et al. (2012, 2014) noted that the modelled absolute and relative abundances of HSE in the Kostomuksha (Puchtel and Humayun, 2000, 2005) and NSB mantle sources, both associated with positive ε^{182}W anomalies, were too similar to that of primitive upper mantle (PUM) to represent a mantle source that is lacking a late veneer contribution. Touboul et al. (2012, 2014) proposed two different models for the two localities studied: for the Kostomuksha source, Touboul et al. (2012) preferred a model invoking an early (>4530 Ma) mantle differentiation event, which post-dated the addition of meteoritic late veneer, but when ^{182}Hf was still extant. For the NSB, Touboul et al. (2014) suggested radiogenic ε^{182}W to be transferred from subducted Hadean sediments into a mantle source enriched in HSE. Instead, we feel that a conceptually simpler rationalisation of the common and global radiogenic ε^{182}W observed in all these Archean rocks can be achieved if the mantle sources supplying these terranes were lacking a late veneer component (Willbold et al., 2011). We admit, however, that our original 2011 model did not consider the HSE abundances in early Archean mantle sources. This was in part because we deemed modelled HSE compositions of Archean mantle sources derived from the inversion of measured HSE data of (often evolved) whole-rock samples to be a less reliable tracer for pre-late veneer mantle than isotopic ε^{182}W data in the same rocks. Nevertheless, we now seek to address this issue specifically. Here, we explore further the question how positive ε^{182}W values found in samples from the AGC, Isua Supracrustal Belt and NSB could be related to a pre-late veneer mantle source given that their sources do not appear to be sufficiently depleted in HSE abundances.

In our first of two possible scenarios, we explore the assumption that the small but significant and systematic offset of ε^{182}W = +0.15 in the pre-late veneer mantle resulted from a combination of core formation process(es) and accretionary impact events on the proto-Earth. A final and pervasive Moon-forming event must eventually have set the ε^{182}W value of the pre-late veneer terrestrial mantle (Münker, 2010; Nimmo et al., 2010; Pahlevan and Stevenson, 2007; Touboul et al., 2007) and also led to the formation of a terrestrial magma ocean (Canup, 2004; Labrosse et al., 2007; Walter et al., 2004). It is as yet unclear to what degree the cores of the proto-Earth and the impactor merged during this event (i.e. see Canup, 2004 and Nimmo et al., 2010) but it is not inconceivable that a small amount of core material became entrained into the proto-Earth's mantle thus affecting its HSE inventory.

Details of the model calculations of this scenario are given in the Supplementary Material and are summarised in Fig. 6. We acknowledge that such a model requires an ε^{182}W > +0.15 for the proto-Earth mantle but recent preliminary high-precision W isotopic analyses of the Moon suggest this is likely the case (Kruijer et al., 2015; Walker et al., 2015). Adding ca. 0.2% of core material back into the proto-Earth mantle after the last metal-silicate equilibration, results in a pre-late veneer mantle with an HSE budget ca. 75% relative to that of PUM as well as an ε^{182}W of +0.15 (Fig. 6). We suggest such entrained core material became quickly homogenised within the pre-late veneer mantle magma ocean. This underpins our observation that the pre-late veneer mantle, as sampled by ca. 4000 Ma old crust from world-wide localities (Fig. 5), appears to have a homogeneous W isotopic composition. We note that a chondritic late veneer is nevertheless required to reconcile the changing ε^{182}W composition from ~4000 Ma to present (see Supplementary Material).

In our second possible scenario (Fig. 7), we investigate the effect of mixing a pre-late veneer mantle reservoir, which became isolated from the remaining mantle in the Hadean (Willbold et al., 2011), with a 'veneered' PUM-like upper mantle on the HSE budget of the resulting mixture (Supplementary Material for details; note that in this scenario we do not envisage the entrainment of core material). Such a mixing process may have operated during the rise of a pre-late veneer reservoir through the Archean mantle if continents were ultimately derived from deep-seated upwellings (see Guitreau et al., 2012) or for the source of the Archean Kostomuksha komatiites (Fig. 5). Our calculations show that entrainment of small amounts of PUM-like material can selectively enriched the pre-late veneer mantle material in HSE and set the HSE ratios close to chondritic values, while retaining characteristically radiogenic ε^{182}W signature.

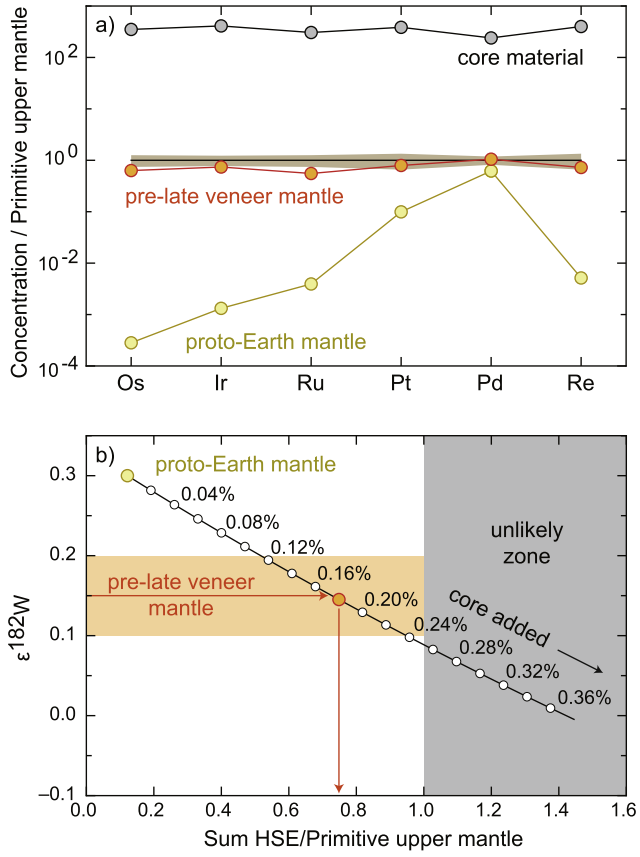

Fig. 6. (a) Expected highly siderophile element (HSE) concentrations in the pre-late veneer mantle as a result of augmenting a proto-Earth mantle with <0.2 wt.% of core material during the Moon-forming impact event. The shaded grey area in (a) represents the uncertainty of HSE concentrations in primitive upper mantle (PUM; Becker et al., 2006). Also shown are the calculated concentrations of HSE-depleted proto-Earth mantle following core formation at lower mantle pressures (40 GPa; Mann et al., 2012) and core material. (b) Such pre-late veneer mantle would be characterised by ε^{182}W of +0.15 and total HSE abundances of ca. 75% relative to PUM. The arrow marks the composition of pre-late veneer mantle shown in (a). Yellow-shaded range represents uncertainty of ε^{182}W in the pre-late veneer mantle. Note that assuming an ε^{182}W value much higher than +0.30 for the proto-Earth's mantle would either yield unrealistically radiogenic ε^{182}W values or too high HSE concentrations in the pre-late veneer mantle (unlikely zone; grey-shaded area). See Supplementary Material for details.

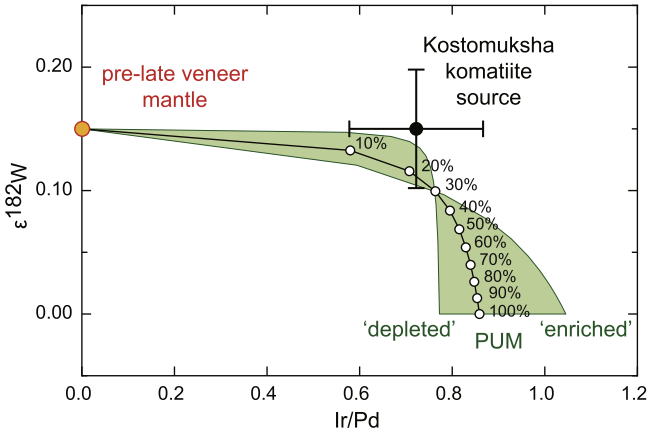

Fig. 7. Expected Ir/Pd ratios and ε^{182}W values in a mixture of pre-late veneer mantle and primitive upper mantle (PUM). The shaded green area represents the effect of variability of Ir and Pd in PUM (Becker et al., 2006) on the mixture. In the 'depleted' model we assume high HSE/W ratios whereas in the 'enriched' case we assume low HSE/W ratios (see Supplementary Material for details). Also shown is the range of Ir/Pd and ε^{182}W values in Kostomuksha komatiites (Puchtel and Humayun, 2005; Touboul et al., 2012). Range of W concentrations in primitive upper mantle taken from Arevelo and McDonough (2008).

5.5. The W isotopic evolution of the Earth's Archean mantle

The finding of radiogenic ε^{182}W of +0.15 in the 2800 Ma Kostomuksha komatiites (Touboul et al., 2012) is inconsistent with a model wherein whole mantle homogenisation of the late veneer material was achieved by ca. 3600 Ma (Fig. 5). Notably, the 2800 Ma Kostomuksha komatiites are characterised by primitive mantle-like ε^{142}Nd ~ 0 (Touboul et al., 2012). Tholeiitic lava flows from the Abitibi Greenstone Belt (Debaille et al., 2013) as well as komatiites from the Belingwe Greenstone Belt (Boyet and Carlson, 2006), all similar in age, display small but significant positive ε^{142}Nd anomalies indicating that the re-mixing of early-formed *silicate* reservoirs within the convecting mantle was not fully completed by ca. 2800 Ma (Debaille et al., 2013; Rizo et al., 2013). We regard it as unlikely that the primitive mantle-like ε^{142}Nd of the Kostomuksha komatiites is a coincidental mixture of an enriched and depleted component within an isotopically heterogeneous Kostomuksha mantle source. Instead, we suggest that the Kostomuksha komatiites probe an Archean mantle source that has not been affected by pervasive silicate differentiation events. In fact, these samples may represent the *pristine* pre-late veneer mantle reservoir that remained isolated from the convecting mantle and so preserved its ε^{182}W composition up to ca. 2800 Ma (Touboul et al., 2012; Figs. 5 and 8). A generic model that could accommodate these observations is a top-to-bottom homogenisation of 'veneered' PUM with pre-late veneer lower mantle during the late Archean (compare with Meier et al., 2009). Recent numerical calculations combined with Hadean zircon ages suggest that impact events related to late accretion could have led to extensive resurfacing of the early Earth's crust (Abramov et al., 2013) and makes burial of the impactors into the deep mantle unlikely (Marchi et al., 2014). This suggests that the late veneer material must have been emplaced into the crust or shallow mantle and progressively mixed into the latter. In such a model, patches of pre-late veneer mantle may have become isolated in the lower mantle until they became successively erased in the late Archean/early Proterozoic by mantle stirring and mixing (Fig. 8).

Although fast mantle stirring times of 100–250 million years have been suggested in the Hadean (Caro et al., 2006; Coltice and Schmalzl, 2006; van Keken and Zhong, 1999) this does not *a prior* exclude the long-term preservation of pre-late veneer mantle within the lower Archean mantle. It is noteworthy that numerical, experimental, chemical and isotopic data (Gonnermann et al., 2002; Samuel and Farnetani, 2003; van der Hilst, 1999) suggest that a heterogeneous lower mantle could have been preserved at least until 3000 Ma. Several recent studies suggest that the Earth's geodynamic framework underwent a pervasive change at ca. 3000 Ma. Using compositional variations of mantle melts through time and rheological constraints of the present-day mantle, Labrosse and Jaupart (2007) postulated a temperature maximum of the Earth's mantle by about 3000 Ma, which they linked to the start of subduction-driven plate teconics involving oceanic plates similar in size to those of today's. While Pujol et al. (2013) link unradiogenic ^{40}Ar/^{36}Ar ratios in <3500 Ma fluid inclusions from the Pilbara craton (Northwest Australia) to rapid crust extraction between 3500 and 2700 Ma, Shirey and Richardson (2011) found that the mineralogical composition of diamond inclusions changed from peridoditic to eclogitic lithologies at ca. 3000 Ma. The latter has been interpreted as the capture of eclogite via subduction and continental collision and may be taken as evidence for a change in the geodynamic framework from rigid plate to modern-style plate tectonic processes. Similarly, Dhuime et al. (2012) and Næraa et al. (2012) noted an apparent net-decrease in the global crustal growth rate at ~3000 Ma, which could also be

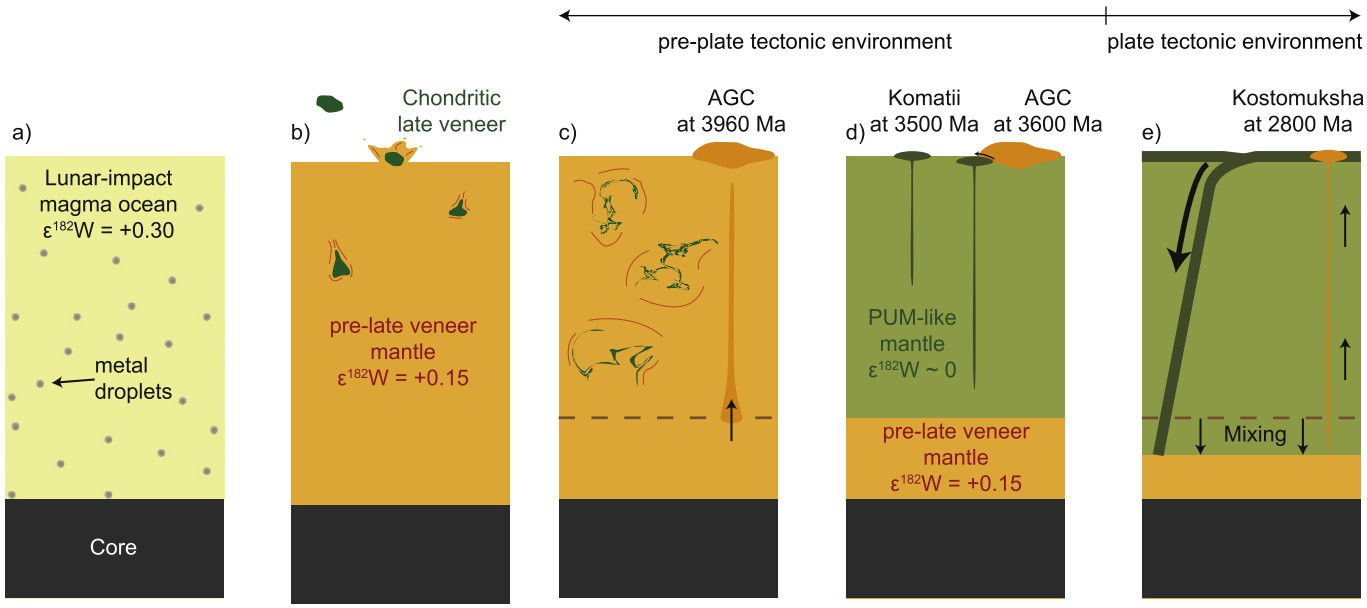

Fig. 8. Illustration of a transient mantle model for the Hadean–Archean Earth (not to scale). (a) During the Moon-forming giant impact core-derived metal droplets mix into the terrestrial magma ocean. (b) The resulting pre-late veneer mantle has $\varepsilon^{182}W = +0.15$ and HSE abundances ca. 80% relative to that of PUM (see Fig. 6). 'Late accretion' added chondritic material ($\varepsilon^{182}W \sim -2$; dark green) as a late veneer to the pre-late veneer mantle. (c) Convective processes in the 'upper' mantle homogenised the mantle with the chondritic late veneer material (green). Owing to the small size of the chondritic components compared to the overall mass of the mantle, the former may not be readily sampled by the Archean rock record. (d) By ca. 3600 Ma top-to-bottom homogenisation of the late veneer material is completed in the mantle except for the lower mantle, which preserved a pre-late veneer $\varepsilon^{182}W$ signature. Addition of new crust to the AGC was sourced in the PUM-like 'veneered' mantle. (e) With the onset of modern plate-tectonic processes at ca. 3000 Ma, the remaining isolated lower mantle reservoir with pristine pre-late veneer $\varepsilon^{182}W$ is destroyed and, in some rare cases, pushed into the upper mantle as mantle plumes to form mantle sources of young, i.e. 2800 Ma, komatiites with positive $\varepsilon^{182}W$ anomalies.

linked to the onset of modern-style subduction-driven plate tectonic processes. We suggest that the contemporaneous increase in $\varepsilon^{182}W$ from ca. 0 to +0.15 between 3000 and 2800 Ma could be a direct response to this change in the geodynamic framework within the Earth's mantle when remnants of pristine pre-late veneer lower mantle became mobilised and possibly pushed to the surface as mantle plumes before finally being destroyed within a fully convecting mantle (Fig. 8e).

6. Conclusions

A range of $\varepsilon^{182}W$ between −0.01 to +0.15 was measured in 3600 to 3960 Ma rocks from the AGC. A correlation between $\varepsilon^{182}W$ and $\varepsilon^{142}Nd$ can be linked to a secondary, in-situ overprint of the short-lived ^{182}W and ^{142}Nd isotope systems during a ca. 3370 Ma tectono-metamorphic event. Samples with the most negative $\varepsilon^{142}Nd$ and most positive $\varepsilon^{182}W$ are assumed to represent the initial isotopic composition of the AGC at the time of its formation at ca. 3960 Ma. Two 3600 Ma samples have $\varepsilon^{182}W$ indistinguishable from the modern terrestrial value. In the three early Archean terranes studied to date (AGC, Isua Supracrustal Belt, NSB), the maximum value of +0.15 $\varepsilon^{182}W$ is constant and in keeping with a pre-late veneer mantle. The $\varepsilon^{182}W$ data for AGC samples suggest that the homogenisation of the late veneer material added to the mantle during this late veneer phase was nearing completion at ca. 3600 in the mantle reservoir that dominated crust formation during most of the Archean.

An isolated Hadean/Archean lower mantle reservoir could have preserved pristine pre-late veneer mantle material. The latter could have gained its characteristic composition as a result of the Moon-forming event and retained its positively anomalous $\varepsilon^{182}W$ signature and high HSE content throughout most of the Archean. It started to mix with the remaining PUM-like mantle when the Earth underwent a transition from a Hadean/Archean proto-plate tectonic mantle system to a post-Archean plate-tectonic system at ca. 3000 Ma. During this shift in the geodynamic framework, distinct 'blobs' of pre-late veneer mantle material rose into the upper mantle and formed mantle sources of late-Archean komatiite suites with positive $\varepsilon^{182}W$ (i.e. the ~2800 Ma Kostomuksha komatiites). Eventually, the lower mantle became fully mixed into the remaining PUM-like mantle resulting in the overall decrease of $\varepsilon^{182}W$ and increase of HSE abundances in the rock record during the late Archean and early Proterozoic.

Acknowledgements

This work benefitted from discussions and debates with W. Bleeker, W. Bottke, N.L. Cates, E.A. Frank, M. Guitreau, A. Morbidelli, K. Pahlevan, A. Roth, M. Touboul, and R. Walker and constructive comments by Thorsten Kleine, an anonymous reviewer and editor Bernard Marty. M.W., H.-W.C. and T.E. gratefully acknowledge funding from NERC (NE/J018031/2 and NE/L004011/1) that made this work possible. T.E. and H.-W.C. also acknowledge funding from the ERC in grant 321209 ISONEB. S.J.M. received funding from the NASA Lunar Science Institute's Center for Lunar Origin and Evolution (CLOE), and the NASA Exobiology Program. A significant portion of this manuscript was completed while S.J.M. held a Distinguished Research Professor chair at the Hungarian Academy of Sciences.

Appendix A. Supplementary material

Supplementary material related to this article can be found online at http://dx.doi.org/10.1016/j.epsl.2015.02.040.

References

Abramov, O., Kring, D.A., Mojzsis, S.J., 2013. The impact environment of the Hadean Earth. Chem. Erde 73, 227–248.
Arevelo, R.J., McDonough, W.F., 2008. Tungsten geochemistry and implications for understanding the Earth's interior. Earth Planet. Sci. Lett. 272, 656–665.
Audétat, A., Günther, D., Heinrich, C.A., 2000. Magmatic-hydrothermal evolution in a fractionating granite: a microchemical study of the Sn–W–F-mineralized Mole Granite (Australia). Geochim. Cosmochim. Acta 64, 3373–3393.

Bali, E., Keppler, H., Audetat, A., 2012. The mobility of W and Mo in subduction zone fluids and the Mo–W–Th–U systematics of island arc magmas. Earth Planet. Sci. Lett. 351–352, 195–207.

Becker, H., Horan, M.F., Walker, R.J., Gao, S., Lorand, J.-P., Rudnick, R.L., 2006. Highly siderophile element composition of the Earth's primitive upper mantle: constraints from new data on peridotite massifs and xenoliths. Geochim. Cosmochim. Acta 70, 4528–4550.

Bennett, V.C., Brandon, A.D., Nutman, A.P., 2007. Coupled ^{142}Nd–^{143}Nd isotopic evidence for Hadean mantle dynamics. Science 318, 1907–1910.

Bleeker, W., Stern, R., 1997. The Acasta gneisses: an imperfect sample of Earth's oldest crust. Lithoprobe Rep. 56, 32–35.

Bottke, W.F., Walker, R.J., Day, J.M.D., Nesvorny, D., Elkins-Tanton, L., 2010. Stochastic late accretion to Earth, the Moon and Mars. Science 330, 1527–1530.

Bowring, S.A., Housh, T., 1995. The Earth's early evolution. Science 269, 1535–1540.

Bowring, S.A., Housh, T.B., Isachsen, C.E., 1990. The Acasta gneisses: remnant of Earth's early crust. In: Newsom, H.E., Jones, J. (Eds.), Origin of the Earth. University Press, Oxford, pp. 319–343.

Boyet, M., Blichert-Toft, J., Rosing, M.T., Storey, M., Télouk, P., Albarède, F., 2003. ^{142}Nd evidence for early Earth differentiation. Earth Planet. Sci. Lett. 214, 427–442.

Boyet, M., Carlson, R.W., 2006. A new geochemical model for the Earth's mantle inferred from ^{146}Sm–^{142}Nd systematics. Earth Planet. Sci. Lett. 250, 254–268.

Canup, R.M., 2004. Simulations of a late lunar-forming impact. Icarus 168, 433–456.

Caro, G., Bourdon, B., Birck, J.-L., Moorbath, S., 2003. ^{146}Sm–^{142}Nd evidence from Isua metamorphosed sediments for early differentiation of the Earth's mantle. Nature 423, 428–432.

Caro, G., Bourdon, B., Birck, J.-L., Moorbath, S., 2006. High-precision ^{142}Nd/^{144}Nd measurements in terrestrial rocks: constraints on the early differentiation of the Earth's mantle. Geochim. Cosmochim. Acta 70, 164–191.

Caro, G., Bourdon, B., Wood, B.J., Corgne, A., 2005. Trace-element fractionation in Hadean mantle generated by melt segregation from a magma ocean. Nature 436, 246–249.

Cates, N.L., Mojzsis, S.J., 2007. Pre-3750 Ma supracrustal rocks from the Nuvvuagittuq supracrustal belt, northern Québec. Earth Planet. Sci. Lett. 255, 9–21.

Chou, C.-L., 1978. Fractionation of siderophile elements in the Earth's upper mantle and lunar samples. In: Proceedings of the 9th Lunar and Planetary Science Conference, pp. 163–165.

Coltice, N., Schmalzl, J., 2006. Mixing times in the mantle of the early Earth derived from 2-D and 3-D numerical simulations of convection. Geophys. Res. Lett. 33, L23304. http://dx.doi.org/10.1029/2006GL027707.

Condie, K.C., 2008. Did the character of subduction change at the end of the Archean? Constraints from convergent-margin granitoids. Geology 36, 611–614.

Davaille, A., 1999. Two-layer thermal convection in miscible viscous fluids. J. Fluid Mech. 379, 223–253.

Debaille, V., O'Neill, C., Brandon, A.D., Haenecour, P., Yin, Q.-Z., Mattielli, N., Treiman, A.H., 2013. Stagnant-lid tectonics in early Earth revealed by ^{142}Nd variations in late Archean rocks. Earth Planet. Sci. Lett. 373, 83–92.

Dhuime, B., Hawkesworth, C.J., Cawood, P.A., Storey, C.D., 2012. A change in the geodynamics of continental growth 3 billion years ago. Science 335, 1334–1336.

Goldschmidt, V.M., 1930. Geochemische Verteilungsgesetze und kosmische Häufigkeiten der Elemente. Naturwissenschaften 18, 999–1013.

Gonnermann, H.M., Manga, M., Mark Jellinek, A., 2002. Dynamics and longevity of an initially stratified mantle. Geophys. Res. Lett. 29. 33-31–33-34.

Guitreau, M., Blichert-Toft, J., Martin, H., Mojzsis, S.J., Albarède, F., 2012. Hafnium isotope evidence from Archean granitic rocks for deep-mantle origin of continental crust. Earth Planet. Sci. Lett. 337–338, 211–223.

Guitreau, M., Blichert-Toft, J., Mojzsis, S.J., Roth, A.S.G., Bourdon, B., Cates, N.L., Bleeker, W., 2014. Lu–Hf isotope systematics of the Hadean-Eoarchean Acasta Gneiss Complex (Northwest Territories, Canada). Geochim. Cosmochim. Acta 135, 251–269.

Harper, C.L., Jacobsen, S.B., 1992. Evidence from coupled ^{147}Sm–^{143}Nd and ^{146}Sm–^{142}Nd systematics for very early (4.5 Gyr) differentiation of the Earth's mantle. Nature 360, 728–732.

Herrington, R., 2011. Geological features and genetic models of mineral deposits. In: Darling, P. (Ed.), SME Mining Engineering Handbook. SME.

Iizuka, T., Horie, K., Komiya, T., Maruyama, S., Hirata, T., Hidaka, H., Windley, B.F., 2006. 4.2 Ga zircon xenocryst in an Acasta gneiss from northwestern Canada: evidence for early continental crust. Geology 34, 245–248.

Iizuka, T., Komiya, T., Johnson, S.P., Kon, Y., Maruyama, S., Hirata, T., 2009. Reworking of Hadean crust in the Acasta gneisses, northwestern Canada: evidence from in-situ Lu–Hf isotope analysis of zircon. Chem. Geol. 259, 230–239.

Iizuka, T., Komiya, T., Ueno, Y., Katayama, I., Uehara, Y., Maruyama, S., Hirata, T., Johnson, S.P., Dunkley, D.J., 2007. Geology and zircon geochronology of the Acasta Gneiss Complex, northwestern Canada: new constraints on its tectonothermal history. Precambrian Res. 153, 179–208.

Iizuka, T., Nakai, S., Sahoo, Y.V., Takamasa, A., Hiraga, T., Maruyama, S., 2010. The tungsten isotopic composition of Eoarchean rocks: implications for early silicate differentiation and core–mantle interaction on Earth. Earth Planet. Sci. Lett. 291, 189–200.

Kellogg, L.H., Turcotte, D.L., 1990. Mixing and the distribution of heterogeneities in a chaotically convecting mantle. J. Geophys. Res. 95, 421–432.

Kleine, T., Münker, C., Mezger, K., Palme, H., 2002. Rapid accretion and early core formation on asteroids and the terrestrial planets from Hf–W chronometry. Nature 418, 952–955.

König, S., Münker, C., Hohl, S., Paulick, H., Barth, A.R., Lagos, M., Pfänder, J., Büchl, A., 2011. The Earth's tungsten budget during mantle melting and crust formation. Geochim. Cosmochim. Acta 75, 2119–2136.

König, S., Münker, C., Schuth, S., Garbe-Schönberg, D., 2008. Mobility of tungsten in subduction zones. Earth Planet. Sci. Lett. 274, 82–92.

Kruijer, T.S., Kleine, T., Fischer-Gödde, M., Sprung, P., 2015. High-precision ^{182}W composition of the Moon: constraints on late accretion and lunar formation models. In: 46th Lunar and Planetary Science Conference, p. 1885.

Labrosse, S., Hernlund, J.W., Coltice, N., 2007. A crystallizing dense magma ocean at the base of the Earth's mantle. Nature 450, 866–869.

Labrosse, S., Jaupart, C., 2007. Thermal evolution of the Earth: secular changes and fluctuations of plate characteristics. Earth Planet. Sci. Lett. 260, 465–481.

Linnen, R.L., Van Lichtervelde, M., Černý, P., 2012. Granitic pegmatites as sources of strategic metals. Elements 8, 275–280.

Mann, U., Frost, D.J., Rubie, D.C., Becker, H., Audétat, A., 2012. Partitioning of Ru, Rh, Pd, Re, Ir and Pt between liquid metal and silicate at high pressures and high temperatures – implications for the origin of highly siderophile element concentrations in the Earth's mantle. Geochim. Cosmochim. Acta 84, 593–613.

Manning, D.A.C., Henderson, P., 1984. The behaviour of tungsten in granitic melt–vapour systems. Contrib. Mineral. Petrol. 86, 286–293.

Marchi, S., Bottke, W.F., Elkins-Tanton, L.T., Bierhaus, M., Wuennemann, K., Morbidelli, A., Kring, D.A., 2014. Widespread mixing and burial of Earth's Hadean crust by asteroid impacts. Nature 511, 578–582.

Martin, H., Moyen, J.-F., 2002. Secular changes in tonalite–trondhjemite–granodiorite composition as markers of the progressive cooling of Earth. Geology 30, 319–322.

Masters, R.L., Ague, J.J., 2005. Regional-scale fluid flow and element mobility in Barrow's metamorphic zones, Stonehaven, Scotland. Contrib. Mineral. Petrol. 150, 1–18.

Meier, M., Barnes, S.J., Campbell, I.H., Fiorentini, M.L., Peltonen, P., Barnes, S.-J., Smithies, R.H., 2009. Progressive mixing of meteoritic veneer into the early Earth's deep mantle. Nature 460, 620–623.

Mojzsis, S.J., Cates, N.L., Caro, G., Trail, D., Abramov, O., Guitreau, M., Blichert-Toft, J., Hopkins, M.D., Bleeker, W., 2014. Component geochronology in the polyphase ca. 3920 Ma Acasta Gneiss. Geochim. Cosmochim. Acta 133, 68–96.

Moorbath, S., Whitehouse, M.J., Kamber, B.S., 1997. Extreme Nd-isotope heterogeneity in the early Archaean – fact or fiction? Case histories from northern Canada and West Greenland. Chem. Geol. 135, 213–231.

Morgan, J.W., 1985. Osmium isotope constraints in Earth's late accretionary history. Nature 317, 703–705.

Morgan, J.W., 1986. Ultramafic xenoliths: clues to Earth's late accretionary history. J. Geophys. Res. 91, 12375–12387.

Moyen, J.-F., Martin, H., 2012. Forty years of TTG research. Lithos 148, 312–336.

Münker, C., 2010. A high field strength element perspective on early lunar differentiation. Geochim. Cosmochim. Acta 74, 7340–7361.

Næraa, T., Scherstén, A., Rosing, M.T., Kemp, A.I.S., Hoffmann, J.E., Kokfelt, T.F., Whitehouse, M.J., 2012. Hafnium isotope evidence for a transition in the dynamics of continental growth 3.2 Gyr ago. Nature 485, 627–630.

Nair, R., Chacko, T., 2008. Role of oceanic plateaus in the initiation of subduction and origin of continental crust. Geology 36, 583–586.

Nimmo, F., O'Brian, D.P., Kleine, T., 2010. Tungsten isotopic evolution during late-stage accretion: constrains on Earth–Moon equilibration. Earth Planet. Sci. Lett. 292, 363–370.

O'Neil, J., Carlson, R.W., Francis, D., Stevenson, R.K., 2008. Neodymium-142 evidence for Hadean mafic crust. Science 321, 1828–1831.

Ordóñez-Calderón, J.C., Polat, A., Fryer, B.J., Gagnon, J.E., Raith, J.G., Appel, P.W.U., 2008. Evidence for HFSE and REE mobility during calc-silicate metasomatism, Mesoarchean (~3075 Ma) Ivisaartoq greenstone belt, southern West Greenland. Precambrian Res. 161, 317–340.

Pahlevan, K., Stevenson, D.J., 2007. Equilibration in the aftermath of the lunar-forming giant impact. Earth Planet. Sci. Lett. 262, 438–449.

Puchtel, I.S., Hofmann, A.W., Mezger, K., Jochum, K.P., Shchipansky, A.A., Samsonov, A.V., 1998. Oceanic plateau model for continental crustal growth in the Archean: a case study from the Kostomuksha greenstone belt, NW Baltic shield. Earth Planet. Sci. Lett. 155, 57–74.

Puchtel, I.S., Humayun, M., 2000. Platinum group elements in Kostomuksha komatiites and basalts: implications for oceanic crust recycling and core–mantle interaction. Geochim. Cosmochim. Acta 64, 4227–4242.

Puchtel, I.S., Humayun, M., 2005. Highly siderophile element geochemistry of Os-187-enriched 2.8 Ga Kostomuksha komatiites, Baltic shield. Geochim. Cosmochim. Acta 69, 1607–1618.

Puchtel, I.S., Walker, R.J., Touboul, M., Nisbet, E.G., Byerly, G.R., 2014. Insights into early Earth from the Pt–Re–Os isotope and highly siderophile element abundance systematics of Barberton komatiites. Geochim. Cosmochim. Acta 125, 394–413.

Pujol, M., Marty, B., Burgess, R., Turner, G., Philippot, P., 2013. Argon isotopic composition of Archaean atmosphere probes early Earth geodynamics. Nature 498, 87–90.

Raith, J.G., Prochaska, W., 1995. Tungsten deposits in the Wolfram Schist, Namaqualand, South Africa: strata-bound versus granite-related genetic concepts. Econ. Geol. 90, 1934–1954.
Rizo, H., Boyet, M., Blichert-Toft, J., O'Neil, J., Rosing, M.T., Paquette, J.-L., 2012. The elusive Hadean enriched reservoir revealed by ^{142}Nd deficits in Isua Archaean rocks. Nature 491, 96–100.
Rizo, H., Boyet, M., Blichert-Toft, J., Rosing, M., 2011. Combined Nd and Hf isotope evidence for deep-seated source of Isua lavas. Earth Planet. Sci. Lett. 312, 267–279.
Rizo, H., Boyet, M., Blichert-Toft, J., Rosing, M.T., 2013. Early mantle dynamics inferred from ^{142}Nd variations in Archean rocks from southwest Greenland. Earth Planet. Sci. Lett. 377–378, 324–335.
Roth, A.S.G., Bourdon, B., Mojzsis, S.J., Rudge, J.F., Guitreau, M., Blichert-Toft, J., 2014. Combined ^{147,146}Sm–^{143,142}Nd constraints on the longevity and residence time of early terrestrial crust. Geochem. Geophys. Geosyst. 15, 2329–2345.
Roth, A.S.G., Bourdon, B., Mojzsis, S.J., Touboul, M., Sprung, P., Guitreau, M., Blichert-Toft, J., 2013. Inherited ^{142}Nd anomalies in Eoarchean protoliths. Earth Planet. Sci. Lett. 361, 50–57.
Samuel, H., Farnetani, C.G., 2003. Thermochemical convection and helium concentrations in mantle plumes. Earth Planet. Sci. Lett. 207, 39–56.
Schoenberg, R., Kamber, B.S., Collerson, K.D., Eugster, O., 2002. New W-isotope evidence for rapid terrestrial accretion and very early core formation. Geochim. Cosmochim. Acta 66, 3151–3160.
Shirey, S.B., Richardson, S.H., 2011. Start of the Wilson cycle at 3 Ga shown by diamonds from subcontinental mantle. Science 333, 434–436.
Smithies, R.H., Champion, D.C., Van Kranendonk, M.J., Howard, H.M., Hickman, A.H., 2005. Modern-style subduction processes in the Mesoarchean: geochemical evidence from the 3.12 Ga Whundo intra-oceanic arc. Earth Planet. Sci. Lett. 231, 221–237.
Smithies, R.H., Van Kranendonk, M.J., Champion, D.C., 2007. The Mesoarchean emergence of modern-styles subduction. Gondwana Res. 11, 50–68.
Tera, F., Papanastassiou, D.A., Wasserburg, G.J., 1974. Isotopic evidence for a terminal lunar cataclysm. Earth Planet. Sci. Lett. 22, 1–21.
Touboul, M., Kleine, T., Bourdon, B., Palme, H., Wieler, R., 2007. Late formation and prolonged differentiation of the Moon inferred from W isotopes in lunar metals. Nature 450, 1206–1209.
Touboul, M., Liu, J., O'Neil, J., Puchtel, I.S., Walker, R.J., 2014. New insights into the Hadean mantle revealed by ^{182}W and highly siderophile element abundances of supracrustal rocks from the Nuvvuagittuq Greenstone Belt, Quebec, Canada. Chem. Geol. 383, 63–75.
Touboul, M., Puchtel, I.S., Walker, R.J., 2012. ^{182}W evidence for long-term preservation of early mantle differentiation products. Science 335, 1065–1069.
Touboul, M., Walker, R.J., 2012. High precision tungsten isotope measurement by thermal ionization mass spectrometry. Int. J. Mass Spectrom., 109–117.
van der Hilst, R.D., 1999. Compositional heterogeneity in the bottom 1000 kilometers of Earth's Mantle: toward a hybrid convection model. Science 283, 1885–1888.
van Keken, P., Zhong, S., 1999. Mixing in a 3D spherical model of present-day mantle convection. Earth Planet. Sci. Lett. 171, 533–547.
Van Kranendonk, M.J., 2007. Tectonics of early Earth. In: Van Kranendonk, M.J., Smithies, R.H., Bennett, V.C. (Eds.), Earth's Oldest Rocks. Elsevier, pp. 1105–1116.
Van Kranendonk, M.J., Smithies, R.H., Hickman, A.H., Champion, D.C., 2007a. Paleoarchean development of a continental nucleus: the East Pilbara terrane of the Pilbara craton, Western Australia. In: Van Kranendonk, M.J., Smithies, R.H., Bennett, V.C. (Eds.), Earth's Oldest Rocks. Elsevier, pp. 307–337.
Van Kranendonk, M.J., Smithies, R.H., Hickman, A.H., Champion, D.C., 2007b. Review: secular tectonic evolution of Archean continental crust: interplay between horizontal and vertical processes in the formation of the Pilbara Craton, Australia. Terra Nova 19, 1–38.
Vockenhuber, C., Oberli, F., Bichler, M., Ahmad, I., Quitté, G., Meier, M., Halliday, A.N., Lee, D.-C., Kutschera, W., Steier, P., Gehrke, R.J., Helmer, R.G., 2004. New half-life measurement of ^{182}Hf: improved chronometer for the early Solar system. Phys. Rev. Lett. 93, 172501.
Walker, R.J., 2009. Highly siderophile elements in the Earth, Moon and Mars: update and implications for planetary accretion and differentiation. Chem. Erde 69, 101–125.
Walker, R.J., Touboul, M., Puchtel, I.S., 2015. Tungsten iostope constraints on big events in Earth–Moon history: current insights and limitations. In: 46th Lunar and Planetary Science Conference, p. 1857.
Walter, M.J., Nakamura, E., Trønnes, R.G., Frost, D.J., 2004. Experimental constraints on crystallization differentiation in a deep magma ocean. Geochim. Cosmochim. Acta 68, 4267–4284.
Whitehouse, M.J., Nägler, T.F., Moorbath, S., Kramers, J.D., Kamber, B.S., Frei, R., 2001. Priscoan (4.00 ± 4.03 Ga) orthogneisses from northwestern Canada – by Samuel A. Bowring and Ian S. Williams: discussion. Contrib. Mineral. Petrol. 141, 248–250.
Willbold, M., Elliott, T., Moorbath, S., 2011. The tungsten isotopic composition of the Earth's mantle before the terminal bombardment. Nature 477, 195–198.
Willbold, M., Hegner, E., Stracke, A., Rocholl, A., 2009. Continental geochemical signatures in dacites from Iceland and implications for models of early Archaean crust formation. Earth Planet. Sci. Lett. 279, 44–52.
Yin, Q., Jacobsen, S.B., Yamashita, K., Blichert-Toft, J., Télouk, P., Albarède, F., 2002. A short timescale for terrestrial planet formation from Hf–W chronometry of meteorites. Nature 418, 949–952.